JAERI-M
90-012

NEANDC(J)-147/U
INDC(JPN)-134/L

EVALUATION OF NEUTRON NUCLEAR DATA FOR ^{16}O

February 1990

Keiichi SHIBATA, Tetsuo ASAMI,[*1] Toru MURATA,[*2] Yukinori KANDA[*3]
Satoshi CHIBA, Yutaka NAKAJIMA and Shigeya TANAKA[*4]

日本原子力研究所
Japan Atomic Energy Research Institute

JAERI-M レポートは，日本原子力研究所が不定期に公刊している研究報告書です。
入手の問合わせは，日本原子力研究所技術情報部情報資料課（〒319-11茨城県那珂郡東海村）あて，お申しこしください。なお，このほかに財団法人原子力弘済会資料センター（〒319-11 茨城県那珂郡東海村日本原子力研究所内）で複写による実費頒布をおこなっております。

JAERI-M reports are issued irregularly.
Inquiries about availability of the reports should be addressed to Information Division Department of Technical Information, Japan Atomic Energy Research Institute, Tokai-mura, Naka-gun, Ibaraki-ken 319-11, Japan.

編集兼発行　日本原子力研究所
印　　刷　いばらき印刷㈱

JAERI-M 90-012

Evaluation of Neutron Nuclear Data for ^{16}O

Keiichi SHIBATA, Tetsuo ASAMI*1, Toru MURATA*2, Yukinori KANDA*3
Satoshi CHIBA, Yutaka NAKAJIMA and Shigeya TANAKA*4

Japanese Nuclear Data Committee
Tokai Research Establishment
Japan Atomic Energy Research Institute
Tokai-mura, Naka-gun, Ibaraki-ken

(Received January 18, 1990)

Neutron nuclear data of ^{16}O have been evaluated for JENDL-3 in the energy range from 10^{-5} eV to 20 MeV. Evaluated quantities are the total, elastic and inelastic scattering, (n,2n), (n,γ), (n,p), (n,d), (n,α), (n,np) and (n,nα) reaction cross sections and the angular and energy distributions of emitted neutrons and gamma-rays. The total cross section below 3 MeV was calculated on the basis of the R-matrix theory. The inelastic scattering, (n,np) and (n,nα) reaction cross sections were obtained from the statistical model calculation. The gamma-ray production cross section was also calculated with the statistical model.

Keywords: Evaluation, Neutron Nuclear Data, Oxygen-16, Cross Section, JENDL-3, R-Matrix Theory, Statistical Model

---

This work was performed as an activity of Working Group on Nuclear Data for Fusion, Japanese Nuclear Data Committee.

*1 Nuclear Energy Data Center
*2 TOSHIBA, Ltd.
*3 Interdisciplinary Graduate School of Engineering Sciences, Kyushu University
*4 O-u College

^{16}Oの中性子核データの評価

日本原子力研究所東海研究所
シグマ研究委員会
柴田　恵一・浅見　哲夫[*1]・村田　徹[*2]・神田　幸則[*3]
千葉　敏・中島　豊・田中　茂也[*4]

（1990年1月18日受理）

^{16}Oの中性子核データをJENDL－3のために10^{-5}eVから20 MeVのエネルギー範囲で評価した。評価した物理量は，全断面積，弾性・非弾性散乱断面積，(n, 2n)，(n, γ)，(n, p)，(n, d)，(n, α)，(n, np)，(n, nα) 反応断面積および放出中性子，ガンマ線の角度，エネルギー分布である。3 MeV以下の全断面積はR行列理論により評価を行った。非弾性散乱，(n, np)，(n, nα) 反応断面積およびガンマ線生成断面積は，統計理論により計算した。

本報告書は，シグマ研究委員会核融合核データワーキング・グループの活動の成果である。

東海研究所：〒319－11 茨城県那珂郡東海村白方字白根2－4
＊1　(財) 原子力データセンター
＊2　東芝 (株)
＊3　九州大学大学院総合理工学研究科
＊4　奥羽大学

Contents

1. Introduction 1
2. Total Cross Section 2
3. Elastic Scattering Cross Section 3
4. Inelastic Scattering Cross Section 3
5. (n,2n) Reaction Cross Section 5
6. (n,γ) Reaction Cross Section 5
7. (n,p) Reaction Cross Section 6
8. (n,d) Reaction Cross Section 6
9. (n,α) Reaction Cross Section 6
10. (n,nα) and (n,np) Reaction Cross Sections 6
11. Gamma-ray Production Cross Section 7
12. Concluding Remarks 7
Acknowledgments 7
References 8

目　　次

1. はじめに 1
2. 全断面積 2
3. 弾性散乱断面積 3
4. 非弾性散乱断面積 3
5. (n, 2n) 反応断面積 5
6. (n, γ) 反応断面積 5
7. (n, p) 反応断面積 6
8. (n, d) 反応断面積 6
9. (n, α) 反応断面積 6
10. (n, nα) および (n, np) 反応断面積 6
11. ガンマ線生成断面積 7
12. 結　言 7
謝　辞 7
参考文献 8

1. Introduction

Neutron nuclear data of ^{16}O are important for fission reactor and shielding calculations, because oxide fuel is widely used and many shielding materials, for example concrete or water, contain a large amount of oxygen. Furthermore, from the viewpoint of fusion neutronics, they are needed since lithium-oxide has been proposed as a solid-state tritium-breeding material. However, the data of ^{16}O were not included in the second version of Japanese Evaluated Nuclear Data Library, JENDL-2, which was released in December 1982. Under such a situation, we were requested to prepare the evaluated data set including ^{6}Li, ^{7}Li, ^{9}Be, ^{12}C, ^{16}O, Cr, Fe and Ni for analyses of the Japan-USA joint experiment on fusion neutronics using the Fusion Neutronics Source (FNS) facility at JAERI. Thus, we decided to evaluate the data of ^{16}O both for the third version of JENDL, JENDL-3, and for the analyses of the FNS experiment.

The possible neutron-induced reactions below 20 MeV are given in Table 1. Among the reactions, the cross sections for the (n,t), (n,^{3}He) and (n,2α) reactions are expected to be very small, and thus they are neglected in the present evaluation.

This report describes the procedure and the results of the evaluation. The status of the presently evaluated quantities is listed in Table 2.

2. Total Cross Section

The total cross section below 3 MeV was calculated with the R-matrix theory by using the computer code RESCAL[1]. In the calculation, only the elastic scattering channel was taken into consideration. Initial guess-values of the R-matrix parameters were taken from the analysis of Hickey et al.[2] Using the try-and-error method, the final values of parameters were obtained so as to give the best fit to the experimental data[3-7], and they are given in Table 3. The calculated thermal scattering cross section is 3.78 barns, and this value is in good agreement with the value of 3.761 ± 0.006 barns recommended by Mughabghab et al.[8] After the R-matrix calculation, the cross section was corrected for the (n,γ) reaction cross section described in the following section, because the (n,γ) reaction was not considered in the calculation.

Figures 1 and 2 show the calculated results together with the experimental data. As seen in Fig. 2, there exists a window around 2.35 MeV. In the resonance theory, the scattering phase shift is given by

$$\delta_\ell = \delta_\ell^{RES} - \phi_\ell ,$$

where δ_ℓ^{RES} is the resonance scattering phase-shift and $-\phi_\ell$ the hard-sphere scattering phase-shift. In the case of the s-wave scattering, ϕ_ℓ can be expressed by ka, where k is the wave number and a the nuclear radius. At the resonance energy, δ_ℓ^{RES} is, of course, given by

$$\delta_\ell^{RES} = (n + \tfrac{1}{2})\pi, \quad (n=0, \pm1, \pm2, \ldots\ldots),$$

and ϕ_ℓ happens to be nearly equal to $\pi/2$ at an incident energy of 2.35 MeV with a = 4.92 fm. Therefore, a minimum of the cross section appears at 2.35 MeV.

Above 3 MeV, Cierjacks et al.[9] presented a large amount of experimental data with high resolution, and we used their data for the present evaluation. The evaluated data were obtained with the spline-function fitting using the Neutron Data Evaluation System (NDES)[10]. In Figs. 3 and 4, are shown the present results.

3. Elastic Scattering Cross Section

The elastic scattering cross section was obtained by subtracting the reaction cross section from the total cross section. The results are shown in Figs. 5 and 6.

The angular distribution was calculated by RESCAL[1] below 3 MeV. Between 5 and 9 MeV it was also calculated with the resonance theory[11]. The experimental data of Lister and Sayres[12] were used between 3 and 5 MeV, and those of Glendinning et al.[13] were used between 9 and 15 MeV. Above 15 MeV, the distribution was calculated with the spherical optical-model using the potential parameters described in the next section.

4. Inelastic Scattering Cross Section

The inelastic scattering cross section was calculated with the Hauser-Feshbach theory[14], using the computer code CASTHY[15]. The level scheme of ^{16}O was taken from the compilation of Ajzenberg-Selove[16], and it is given in Table 4. Above 14.4 MeV, overlapping levels were assumed, and a constant temperature of 3.4 MeV was obtained from the staircase plot.

As for the optical potential parameters we tried two sets: the parameters of Glendinning et al.[13] and of Gould et al.[17] Using the parameters of Glendinning et al., the calculations gave large cross

Above 3 MeV, Cierjacks et al.[9] presented a large amount of experimental data with high resolution, and we used their data for the present evaluation. The evaluated data were obtained with the spline-function fitting using the Neutron Data Evaluation System (NDES)[10]. In Figs. 3 and 4, are shown the present results.

3. Elastic Scattering Cross Section

The elastic scattering cross section was obtained by subtracting the reaction cross section from the total cross section. The results are shown in Figs. 5 and 6.

The angular distribution was calculated by RESCAL[1] below 3 MeV. Between 5 and 9 MeV it was also calculated with the resonance theory[11]. The experimental data of Lister and Sayres[12] were used between 3 and 5 MeV, and those of Glendinning et al.[13] were used between 9 and 15 MeV. Above 15 MeV, the distribution was calculated with the spherical optical-model using the potential parameters described in the next section.

4. Inelastic Scattering Cross Section

The inelastic scattering cross section was calculated with the Hauser-Feshbach theory[14], using the computer code CASTHY[15]. The level scheme of ^{16}O was taken from the compilation of Ajzenberg-Selove[16], and it is given in Table 4. Above 14.4 MeV, overlapping levels were assumed, and a constant temperature of 3.4 MeV was obtained from the staircase plot.

As for the optical potential parameters we tried two sets: the parameters of Glendinning et al.[13] and of Gould et al.[17] Using the parameters of Glendinning et al., the calculations gave large cross

Above 3 MeV, Cierjacks et al.[9] presented a large amount of experimental data with high resolution, and we used their data for the present evaluation. The evaluated data were obtained with the spline-function fitting using the Neutron Data Evaluation System (NDES)[10]. In Figs. 3 and 4, are shown the present results.

3. Elastic Scattering Cross Section

The elastic scattering cross section was obtained by subtracting the reaction cross section from the total cross section. The results are shown in Figs. 5 and 6.

The angular distribution was calculated by RESCAL[1] below 3 MeV. Between 5 and 9 MeV it was also calculated with the resonance theory[11]. The experimental data of Lister and Sayres[12] were used between 3 and 5 MeV, and those of Glendinning et al.[13] were used between 9 and 15 MeV. Above 15 MeV, the distribution was calculated with the spherical optical-model using the potential parameters described in the next section.

4. Inelastic Scattering Cross Section

The inelastic scattering cross section was calculated with the Hauser-Feshbach theory[14], using the computer code CASTHY[15]. The level scheme of ^{16}O was taken from the compilation of Ajzenberg-Selove[16], and it is given in Table 4. Above 14.4 MeV, overlapping levels were assumed, and a constant temperature of 3.4 MeV was obtained from the staircase plot.

As for the optical potential parameters we tried two sets: the parameters of Glendinning et al.[13] and of Gould et al.[17] Using the parameters of Glendinning et al., the calculations gave large cross

sections as compared with the (n,n'γ) data measured by Nordborg et al.[18] On the other hand, the calculations with the parameters of Gould et al. are almost consistent with the (n,n'γ) data. In order to obtain the best agreement between the calculated and measured data, the imaginary potential depth of Gould et al. was a little adjusted. The final values of the parameters used in the present evaluation are given as follows:

$$V = 48.25 - 0.053 \times E_n, \quad W_s = 3.0 + 0.25 \times E_n, \quad V_{so} = 5.5 \text{ (MeV)}$$

$$r_0 = 1.255, \quad r_s = 1.352, \quad r_{so} = 1.15 \text{ (fm)}$$

$$a = 0.536, \quad b = 0.205, \quad a_{so} = 0.5 \text{ (fm)}$$

Up to the fifth level, the cross sections were normalized to the experimental data[19-22] at 14 MeV. Concerning the second and third levels, the structure of cross sections was traced from the (n,n'γ) data[18,23] Furthermore, the cross sections from the sixth to seventeenth levels were normalized so as to reproduce the measured neutron emission spectra[22,24] at 14 MeV. Figure 7 shows the evaluated total inelastic scattering cross section, together with the ENDF/B-IV data.

The angular distributions of neutrons inelastically scattered to the first, second and fifth levels were obtained from the experimental data of Baba et al.[22] As for the third and fourth levels, we adopted the ENDF/B-IV data in the present evaluation. The angular distributions for the inelastic scattering to the rest of discrete levels were calculated with the Hauser-Feshbach theory using the CASTHY code. Isotropic distributions for the overlapping levels

given in the center-of-mass system were transformed into the ones in the laboratory system.

The energy distributions of neutrons inelastically scattered to the overlapping levels were assumed to be evaporation spectra with a constant temperature of 3.4 MeV.

The calculated neutron emission spectra are compared with the measurements of Baba et al.[22] at 14 MeV in Figs. 8-11. The agreement between the evaluated and measured data is satisfactory.

5. (n,2n) Reaction Cross Section

The (n,2n) reaction cross section was evaluated on the basis of the data measured by Brill et al.[25], and it is shown in Fig. 12.

The angular distribution of neutrons emitted from the (n,2n) reaction was assumed to be isotropic in the laboratory system. As to the energy distribution, a simple evaporation spectrum was adopted. The same nuclear temperature was employed as that of ^{7}Li deduced by Chiba et al.[26], and its incident-energy dependence was assumed to be proportional to $(E_n)^{1/2}$.

6. (n,γ) Reaction Cross Section

As the thermal cross section we adopted a value of 0.19 mb recommended by Mughabghab et al.[8] The cross section was extrapolated as $1/v$ up to 20 MeV:

$$\sigma_{n,\gamma} = 3.02 \times 10^{-5} \, [E_n(\mathrm{eV})]^{-1/2} \text{ barns.}$$

The present result is illustrated in Fig. 13. The evaluated cross section is in good agreement with the measurements of Allen and

given in the center-of-mass system were transformed into the ones in the laboratory system.

The energy distributions of neutrons inelastically scattered to the overlapping levels were assumed to be evaporation spectra with a constant temperature of 3.4 MeV.

The calculated neutron emission spectra are compared with the measurements of Baba et al.[22] at 14 MeV in Figs. 8-11. The agreement between the evaluated and measured data is satisfactory.

5. (n,2n) Reaction Cross Section

The (n,2n) reaction cross section was evaluated on the basis of the data measured by Brill et al.[25], and it is shown in Fig. 12.

The angular distribution of neutrons emitted from the (n,2n) reaction was assumed to be isotropic in the laboratory system. As to the energy distribution, a simple evaporation spectrum was adopted. The same nuclear temperature was employed as that of ^{7}Li deduced by Chiba et al.[26], and its incident-energy dependence was assumed to be proportional to $(E_n)^{1/2}$.

6. (n,γ) Reaction Cross Section

As the thermal cross section we adopted a value of 0.19 mb recommended by Mughabghab et al.[8] The cross section was extrapolated as $1/v$ up to 20 MeV:

$$\sigma_{n,\gamma} = 3.02 \times 10^{-5} \, [E_n(\mathrm{eV})]^{-1/2} \text{ barns.}$$

The present result is illustrated in Fig. 13. The evaluated cross section is in good agreement with the measurements of Allen and

given in the center-of-mass system were transformed into the ones in the laboratory system.

The energy distributions of neutrons inelastically scattered to the overlapping levels were assumed to be evaporation spectra with a constant temperature of 3.4 MeV.

The calculated neutron emission spectra are compared with the measurements of Baba et al.[22] at 14 MeV in Figs. 8-11. The agreement between the evaluated and measured data is satisfactory.

5. (n,2n) Reaction Cross Section

The (n,2n) reaction cross section was evaluated on the basis of the data measured by Brill et al.[25], and it is shown in Fig. 12.

The angular distribution of neutrons emitted from the (n,2n) reaction was assumed to be isotropic in the laboratory system. As to the energy distribution, a simple evaporation spectrum was adopted. The same nuclear temperature was employed as that of ^{7}Li deduced by Chiba et al.[26], and its incident-energy dependence was assumed to be proportional to $(E_n)^{1/2}$.

6. (n,γ) Reaction Cross Section

As the thermal cross section we adopted a value of 0.19 mb recommended by Mughabghab et al.[8] The cross section was extrapolated as $1/v$ up to 20 MeV:

$$\sigma_{n,\gamma} = 3.02 \times 10^{-5} \, [E_n(\mathrm{eV})]^{-1/2} \text{ barns.}$$

The present result is illustrated in Fig. 13. The evaluated cross section is in good agreement with the measurements of Allen and

Macklin[27] at 30 keV. In the higher energy region our evaluation may be inappropriate. However, the cross section is expected to be extremely small in that region, and thus no problem arises practically.

7. (n,p) Reaction Cross Section

The (n,p) reaction cross section was obtained from the measurements of Bormann et al.[28], DeJuren and Stooksberry[29], Seeman and Moore[30] and Martin[31]. The evaluated result is illustrated in Fig. 14.

8. (n,d) Reaction Cross Section

The (n,d) reaction cross section was taken from the evaluation of Foster, Jr. and Young[32], and it is shown in Fig. 15.

9. (n,α) Reaction Cross Section

The (n,α) reaction cross section was evaluated on the basis of the measurements of Nordborg et al.[18], Davis et al.[33], Sick et al.[34], Divatia et al.[35], Dickens and Perey[36], Orphan et al.[37] and Bair and Haas[38]. Figure 16 shows the evaluated (n,α) reaction cross section.

10. (n,nα) and (n,np) Reaction Cross Sections

The cross sections and neutron emission spectra for the (n,nα) and (n,np) reactions were calculated with the statistical model, by using the GNASH code[39]. Figures 17 and 18 show the evaluated results.

Macklin[27] at 30 keV. In the higher energy region our evaluation may be inappropriate. However, the cross section is expected to be extremely small in that region, and thus no problem arises practically.

7. (n,p) Reaction Cross Section

The (n,p) reaction cross section was obtained from the measurements of Bormann et al.[28], DeJuren and Stooksberry[29], Seeman and Moore[30] and Martin[31]. The evaluated result is illustrated in Fig. 14.

8. (n,d) Reaction Cross Section

The (n,d) reaction cross section was taken from the evaluation of Foster, Jr. and Young[32], and it is shown in Fig. 15.

9. (n,α) Reaction Cross Section

The (n,α) reaction cross section was evaluated on the basis of the measurements of Nordborg et al.[18], Davis et al.[33], Sick et al.[34], Divatia et al.[35], Dickens and Perey[36], Orphan et al.[37] and Bair and Haas[38]. Figure 16 shows the evaluated (n,α) reaction cross section.

10. (n,nα) and (n,np) Reaction Cross Sections

The cross sections and neutron emission spectra for the (n,nα) and (n,np) reactions were calculated with the statistical model, by using the GNASH code[39]. Figures 17 and 18 show the evaluated results.

Macklin[27] at 30 keV. In the higher energy region our evaluation may be inappropriate. However, the cross section is expected to be extremely small in that region, and thus no problem arises practically.

7. (n,p) Reaction Cross Section

The (n,p) reaction cross section was obtained from the measurements of Bormann et al.[28], DeJuren and Stooksberry[29], Seeman and Moore[30] and Martin[31]. The evaluated result is illustrated in Fig. 14.

8. (n,d) Reaction Cross Section

The (n,d) reaction cross section was taken from the evaluation of Foster, Jr. and Young[32], and it is shown in Fig. 15.

9. (n,α) Reaction Cross Section

The (n,α) reaction cross section was evaluated on the basis of the measurements of Nordborg et al.[18], Davis et al.[33], Sick et al.[34], Divatia et al.[35], Dickens and Perey[36], Orphan et al.[37] and Bair and Haas[38]. Figure 16 shows the evaluated (n,α) reaction cross section.

10. (n,nα) and (n,np) Reaction Cross Sections

The cross sections and neutron emission spectra for the (n,nα) and (n,np) reactions were calculated with the statistical model, by using the GNASH code[39]. Figures 17 and 18 show the evaluated results.

Macklin[27] at 30 keV. In the higher energy region our evaluation may be inappropriate. However, the cross section is expected to be extremely small in that region, and thus no problem arises practically.

7. (n,p) Reaction Cross Section

The (n,p) reaction cross section was obtained from the measurements of Bormann et al.[28], DeJuren and Stooksberry[29], Seeman and Moore[30] and Martin[31]. The evaluated result is illustrated in Fig. 14.

8. (n,d) Reaction Cross Section

The (n,d) reaction cross section was taken from the evaluation of Foster, Jr. and Young[32], and it is shown in Fig. 15.

9. (n,α) Reaction Cross Section

The (n,α) reaction cross section was evaluated on the basis of the measurements of Nordborg et al.[18], Davis et al.[33], Sick et al.[34], Divatia et al.[35], Dickens and Perey[36], Orphan et al.[37] and Bair and Haas[38]. Figure 16 shows the evaluated (n,α) reaction cross section.

10. (n,nα) and (n,np) Reaction Cross Sections

The cross sections and neutron emission spectra for the (n,nα) and (n,np) reactions were calculated with the statistical model, by using the GNASH code[39]. Figures 17 and 18 show the evaluated results.

Macklin[27] at 30 keV. In the higher energy region our evaluation may be inappropriate. However, the cross section is expected to be extremely small in that region, and thus no problem arises practically.

7. (n,p) Reaction Cross Section

The (n,p) reaction cross section was obtained from the measurements of Bormann et al.[28], DeJuren and Stooksberry[29], Seeman and Moore[30] and Martin[31]. The evaluated result is illustrated in Fig. 14.

8. (n,d) Reaction Cross Section

The (n,d) reaction cross section was taken from the evaluation of Foster, Jr. and Young[32], and it is shown in Fig. 15.

9. (n,α) Reaction Cross Section

The (n,α) reaction cross section was evaluated on the basis of the measurements of Nordborg et al.[18], Davis et al.[33], Sick et al.[34], Divatia et al.[35], Dickens and Perey[36], Orphan et al.[37] and Bair and Haas[38]. Figure 16 shows the evaluated (n,α) reaction cross section.

10. (n,nα) and (n,np) Reaction Cross Sections

The cross sections and neutron emission spectra for the (n,nα) and (n,np) reactions were calculated with the statistical model, by using the GNASH code[39]. Figures 17 and 18 show the evaluated results.

11. Gamma-ray Production Cross Section

The gamma-ray production cross sections and gamma-ray energy spectra were calculated using the GNASH code. The channels included in the calculation are the (n,n'γ), (n,pγ), (n,αγ) and (n,γ) reactions. The gamma-ray transition from the first level of ^{16}O was regarded as strictly forbidden.

12. Concluding Remarks

Evaluation of neutron nuclear data for ^{16}O has been performed in the energy range from 10^{-5} eV to 20 MeV.

In the present evaluation, the total cross section below 3 MeV was obtained from the R-matrix calculation, and the cross section above 3 MeV was evaluated on the basis of the data measured by Cierjacks et al.[9] The inelastic scattering cross sections were mainly calculated with the statistical model taking account of twenty-nine discrete levels, although the cross sections were adjusted so as to reproduce the measured neutron emission spectra at 14 MeV.

The threshold-reaction cross sections such as (n,2n), (n,p), (n,d) and (n,α) were evaluated on the basis of the available experimental data.

The present evaluated data of ^{16}O have been compiled into JENDL-3 in the ENDF-5 format.

Acknowledgments

The authors would like to thank Mr. T. Narita for his aid in making graphs. They are also indebted to Dr. Y. Kikuchi for his reading of the manuscript. Careful typewriting by Miss S. Ishibashi is much appreciated.

11. Gamma-ray Production Cross Section

The gamma-ray production cross sections and gamma-ray energy spectra were calculated using the GNASH code. The channels included in the calculation are the (n,n'γ), (n,pγ), (n,αγ) and (n,γ) reactions. The gamma-ray transition from the first level of ^{16}O was regarded as strictly forbidden.

12. Concluding Remarks

Evaluation of neutron nuclear data for ^{16}O has been performed in the energy range from 10^{-5} eV to 20 MeV.

In the present evaluation, the total cross section below 3 MeV was obtained from the R-matrix calculation, and the cross section above 3 MeV was evaluated on the basis of the data measured by Cierjacks et al.[9] The inelastic scattering cross sections were mainly calculated with the statistical model taking account of twenty-nine discrete levels, although the cross sections were adjusted so as to reproduce the measured neutron emission spectra at 14 MeV.

The threshold-reaction cross sections such as (n,2n), (n,p), (n,d) and (n,α) were evaluated on the basis of the available experimental data.

The present evaluated data of ^{16}O have been compiled into JENDL-3 in the ENDF-5 format.

Acknowledgments

The authors would like to thank Mr. T. Narita for his aid in making graphs. They are also indebted to Dr. Y. Kikuchi for his reading of the manuscript. Careful typewriting by Miss S. Ishibashi is much appreciated.

11. Gamma-ray Production Cross Section

The gamma-ray production cross sections and gamma-ray energy spectra were calculated using the GNASH code. The channels included in the calculation are the (n,n'γ), (n,pγ), (n,αγ) and (n,γ) reactions. The gamma-ray transition from the first level of ^{16}O was regarded as strictly forbidden.

12. Concluding Remarks

Evaluation of neutron nuclear data for ^{16}O has been performed in the energy range from 10^{-5} eV to 20 MeV.

In the present evaluation, the total cross section below 3 MeV was obtained from the R-matrix calculation, and the cross section above 3 MeV was evaluated on the basis of the data measured by Cierjacks et al.[9] The inelastic scattering cross sections were mainly calculated with the statistical model taking account of twenty-nine discrete levels, although the cross sections were adjusted so as to reproduce the measured neutron emission spectra at 14 MeV.

The threshold-reaction cross sections such as (n,2n), (n,p), (n,d) and (n,α) were evaluated on the basis of the available experimental data.

The present evaluated data of ^{16}O have been compiled into JENDL-3 in the ENDF-5 format.

Acknowledgments

The authors would like to thank Mr. T. Narita for his aid in making graphs. They are also indebted to Dr. Y. Kikuchi for his reading of the manuscript. Careful typewriting by Miss S. Ishibashi is much appreciated.

References

1) Komoda S., Shibata K., Chiba S. and Igarasi S.: to be published.

2) Hickey G.T., Firk F.W.K., Holt R.J. and Nath R.: Nucl. Phys., A225, 470 (1974).

3) Okazaki A.: Phys. Rev., 99, 55 (1955).

4) Foster, Jr. D.G. and Glasgow D.W.: Phys. Rev., C3, 576 (1971).

5) Cierjacks S., Forti P., Kopsch D., Kropp L., Nebe J. and Unseld H.: "High Resolution Total Cross Sections between 0.5 and 30 MeV", KFK-1000 (1968).

6) Fowler J.L., Johnson C.H., Haas F.X. and Feezel R.M.: "The Neutron Total Cross Section of ^{16}O and ^{40}Ca", Proc. Third Conf. Neutron Cross Sections and Technology, Knoxville 1971, Vol.1, p.179 (1971).

7) Schwartz R.B., Heaton H.T. and Schrack R.A.: "MeV Total Cross Sections", NBS-MONO-138 (1974).

8) Mughabghab S.F., Divadeenam M. and Holden N.E.: "Neutron Cross Sections Vol.1", Academic Press, 1981.

9) Cierjacks S., Hinterberger F., Schmalz G., Erbe D., Rossen P.V. and Leugers B.: Nucl. Instrum. Meth., 169, 185 (1980).

10) Nakagawa T.: J. At. Energy Soc. Jpn., 22, 559 (1980) [in Japanese].

11) Murata T.: "Analysis of Neutron Cross Section of N-14 and O-16 with an Approximate R-matrix Theory", Proc. Int. Conf. Nuclear Data for Science and Technology, Mito, 1988, p.557 (1988), Saikon Publ.

12) Lister D. and Sayres A.: Phys. Rev., 143, 745 (1966).

13) Glendinning S.G., El-Kadi S., Nelson C.E., Purser F.O., Gould C.R. and Seagondollar L.W.: Nucl. Sci. Eng., 82, 393 (1982).

14) Hauser W. and Feshbach H.: Phys. Rev., 87, 366 (1952).

15) Igarasi S.: J. Nucl. Sci. Technol., 12, 67 (1975).

16) Ajzenberg-Selove F.: Nucl. Phys., A375, 1 (1982).

17) Gould C.R., Dave J. and Walter R.L.: "Scattering of 7- to 15-MeV Neutrons from 1-P Shell Nuclei", Proc. Int. Conf. Nuclear Data for Science and Technology, Antwerp, 1982, p.766 (1983); Dave J.H. and Gould C.R.: Phys. Rev., C28, 2212 (1983).

18) Nordborg C., Nilsson L., Condé H. and Strömberg L.G.: Nucl. Sci. Eng., 66, 75 (1978).

19) McDonald W.J., Robson J.M. and Malcolm R.: Nucl. Phys., 75, 353 (1966).

20) Meier D., Brüllmann M., Jung H. and Marmier P.: Helv. Phys. Acta, 42, 813 (1969).

21) Bauer R.W., Anderson J.D. and Christensen L.J.: Nucl. Phys., 47, 241 (1963).

22) Baba M., Ono M., Yabuta N., Kikuti T. and Hirakawa N.: "Scattering of 14.1-MeV Neutrons from ^{10}B, ^{11}B, C, N, O, F and Si", Proc. Int. Conf. Nuclear Data for Basic and Applied Science, Santa Fe, 1985, p.223, (1986), Gordon and Breach.

23) Lundberg B., Strömberg L.G. and Condé H.: Phys. Scr., 2, 273 (1970).

24) Takahashi A., Yamamoto J., Oshima K., Ueda M., Fukazawa M., Yanagi Y., Miyaguchi J. and Sumita K.: J. Nucl. Sci. Technol., 21, 577 (1984).

25) Brill O.D., Vlasov N.A., Kalinin S.P. and Sokolov L.S.: Sov. Phys. Doklady, 6, 24 (1961).

26) Chiba S., Baba M., Nakashima H., Ono M., Yabuta N., Yukinori S. and Hirakawa N.: J. Nucl. Sci. Technol., 22, 771 (1985).

27) Allen B.J. and Macklin R.L.: Phys. Rev., C3, 1737 (1971).

28) Bormann M., Dreyer F., Neuert H., Riehle I. and Zielinski U.: "Measurements of Some Fast Neutron Cross Sections with the Activation Method", Proc. First IAEA Conf. Nuclear Data for Reactors, Paris, 1966, p.225, (1967).

29) DeJuren J.A. and Stooksberry R.W.: Phys. Rev., 127, 1229 (1962).

30) Seeman K.W. and Moore W.E.: Bull. Am. Phys., 6, 237 (1961).

31) Martin H.C.: Phys. Rev., 93, 498 (1954).

32) Foster, Jr. D.G. and Young P.G.: "A Preliminary Evaluation of the Neutron and Photon-Production Cross Sections of Oxygen", LA-4780 (1972).

33) Davis E.A., Bonner T.W., Worley, Jr. D.W. and Bass R.: Nucl. Phys., 48, 169 (1963).

34) Sick I., Baumgartner E., Huber P. and Stammbach Th.: Helv. Phys. Acta, 41, 573 (1968).

35) Divatia A.S., Sekharan K.K., Mehta M.K., Kerekate S.S. and Nambiar K.K.: "$^{16}O(n,\alpha)^{13}C$ Cross Sections from the $^{13}C(\alpha,n)^{16}O$ Reaction", Proc. First IAEA Conf. Nuclear Data for Reactors, Paris, 1966, p.233, (1967).

36) Dickens J.K. and Perey F.G.: Nucl. Sci. Eng., 40, 283 (1970).

37) Orphan V.J., Hoot C.G. and John J.: Nucl. Sci. Eng., 42, 352 (1970).

38) Bair J.K. and Haas F.X.: Phys. Rev., C7, 1356 (1973).

39) Young P.G. and Arthur E.D.: "GNASH: A Preequilibrium, Statistical Nuclear-Model Code for Calculation of Cross Sections and Emission Spectra", LA-6947 (1977).

Table 1 Reaction Q-values and threshold energies.

Reaction	Q-value (MeV)	Threshold (MeV)
$^{16}O(n,\gamma)^{17}O$	4.14460	0.0
$^{16}O(n,p)^{16}N$	- 9.63620	10.2439
$^{16}O(n,d)^{15}N$	- 9.90100	10.5254
$^{16}O(n,t)^{14}N$	-14.4790	15.3921
$^{16}O(n,^{3}He)^{14}C$	-14.6168	15.5386
$^{16}O(n,\alpha)^{13}C$	- 2.2155	2.35521
$^{16}O(n,2n)^{15}O$	-15.6641	16.6519
$^{16}O(n,2\alpha)^{9}Be$	-12.8635	13.6747

Table 2 Status of presently evaluated quantities

Quantities	Energy Range (eV)*		Comments
	Min.	Max.	
a) Cross sections			
Total	1.0 - 5	2.0 + 7	Figs. 1 ~ 4
Elastic scattering	1.0 - 5	2.0 + 7	Figs. 5, 6
Inelastic scattering	6.43 + 6	2.0 + 7	Figs. 7 ~ 11
(n,2n) reaction	1.67 + 7	2.0 + 7	Fig. 12
(n,nα) reaction	7.61 + 6	2.0 + 7	Fig. 17
(n,np) reaction	1.29 + 7	2.0 + 7	Fig. 18
(n,γ) reaction	1.0 - 5	2.0 + 7	Fig. 13
(n,p) reaction	1.02 + 7	2.0 + 7	Fig. 14
(n,d) reaction	1.05 + 7	2.0 + 7	Fig. 15
(n,α) reaction	2.36 + 6	2.0 + 7	Fig. 16
b) Angular distributions of secondary neutrons			
Elastic scattering	1.0 - 5	2.0 + 7	
Inelastic scattering	6.43 + 6	2.0 + 7	
(n,2n) reaction	1.67 + 7	2.0 + 7	
(n,nα) reaction	7.61 + 6	2.0 + 7	
(n,np) reaction	1.29 + 7	2.0 + 7	
c) Energy distributions of secondary neutrons			
Inelastic scattering to continuum	1.53 + 7	2.0 + 7	
(n,2n) reaction	1.67 + 7	2.0 + 7	
(n,nα) reaction	7.61 + 6	2.0 + 7	
(n,np) reaction	1.29 + 7	2.0 + 7	
d) Photon production cross sections			
Inelastic scattering	6.52 + 6	2.0 + 7	
(n,γ) reaction	1.0 - 5	2.0 + 7	
(n,p) reaction	1.04 + 7	2.0 + 7	
(n,α) reaction	5.64 + 6	2.0 + 7	

* 2.0 + 7 denotes 2.0×10^7.

Table 3 R-matrix parameters used in the n + ^{16}O analysis.

ℓ	$J\pi$	$E_\lambda^{J\pi}$ (MeV)	$\gamma_{\lambda n}^{J\pi}$ (MeV$^{1/2}$)	$R_{n0}^{\infty J\pi}$	$R_{n1}^{\infty J\pi}$ (MeV^{-1})	$B^{J\pi}$
0	1/2+	-3.080	0.678	0.0	0.0	0.0
		2.212	0.215			
		3.821	0.228			
1	1/2-	-1.024	0.480	0.380	0.090	-0.337
		1.786	0.140			
		3.900	0.219			
1	3/2-	0.377	0.390	0.540	0.0	-0.405
		1.228	0.173			
		3.242	0.463			
2	3/2+	0.620	0.955	0.20	0.08	-1.194
		1.723	0.118			
		3.106	0.412			
		3.915	0.110			
2	5/2+	-3.899	0.894	0.0	0.0	-0.787
3	7/2-	1.553	0.300	0.500	0.0	-2.600

Channel radius: a = 4.92 fm.

The R-matrix is given by

$$R_{c',c}^{J\pi} = R_c^{\infty J\pi}\delta_{c',c} + \sum_\lambda \gamma_{\lambda c'}^{J\pi}\gamma_{\lambda c}^{J\pi}/(E_\lambda^{J\pi} - E),$$

where

$$R_c^{\infty J\pi} = R_{c0}^{\infty J\pi} + R_{c1}^{\infty J\pi}\cdot E_n.$$

Table 4 Level scheme of ^{16}O.

No.	E_x (MeV)	I^π	No.	E_x (MeV)	I^π
G.S.	0.0	0^+	15	12.440	1^-
1	6.0490	0^+	16	12.530	2^-
2	6.1300	3^-	17	12.800	0^-
3	6.9170	2^+	18	12.970	2^-
4	7.1169	1^-	19	13.020	2^+
5	8.8720	2^-	20	13.090	1^-
6	9.6300	1^-	21	13.120	3^-
7	9.8470	2^+	22	13.260	3^-
8	10.360	4^+	23	13.660	1^+
9	10.960	0^-	24	13.870	4^+
10	11.080	3^+	25	13.980	2^-
11	11.100	4^+	26	14.030	0^+
12	11.520	2^+	27	14.100	3^-
13	11.600	3^-	28	14.300	4^+
14	12.050	0^+	29	14.400	5^+

Levels above 14.4 MeV are assumed to be overlapping.

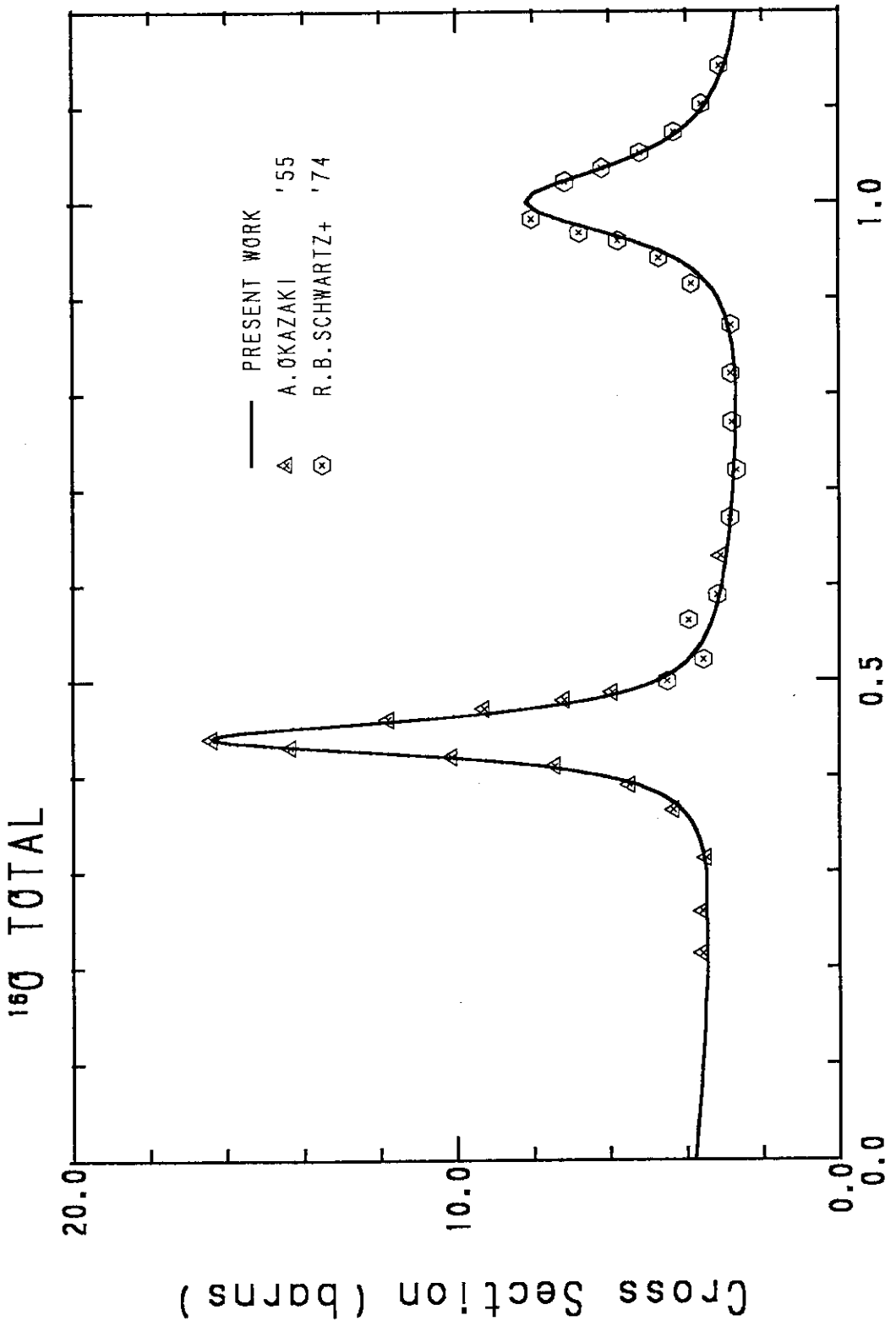

Fig. 1 Measured and evaluated total cross sections of ^{16}O below 1.2 MeV.

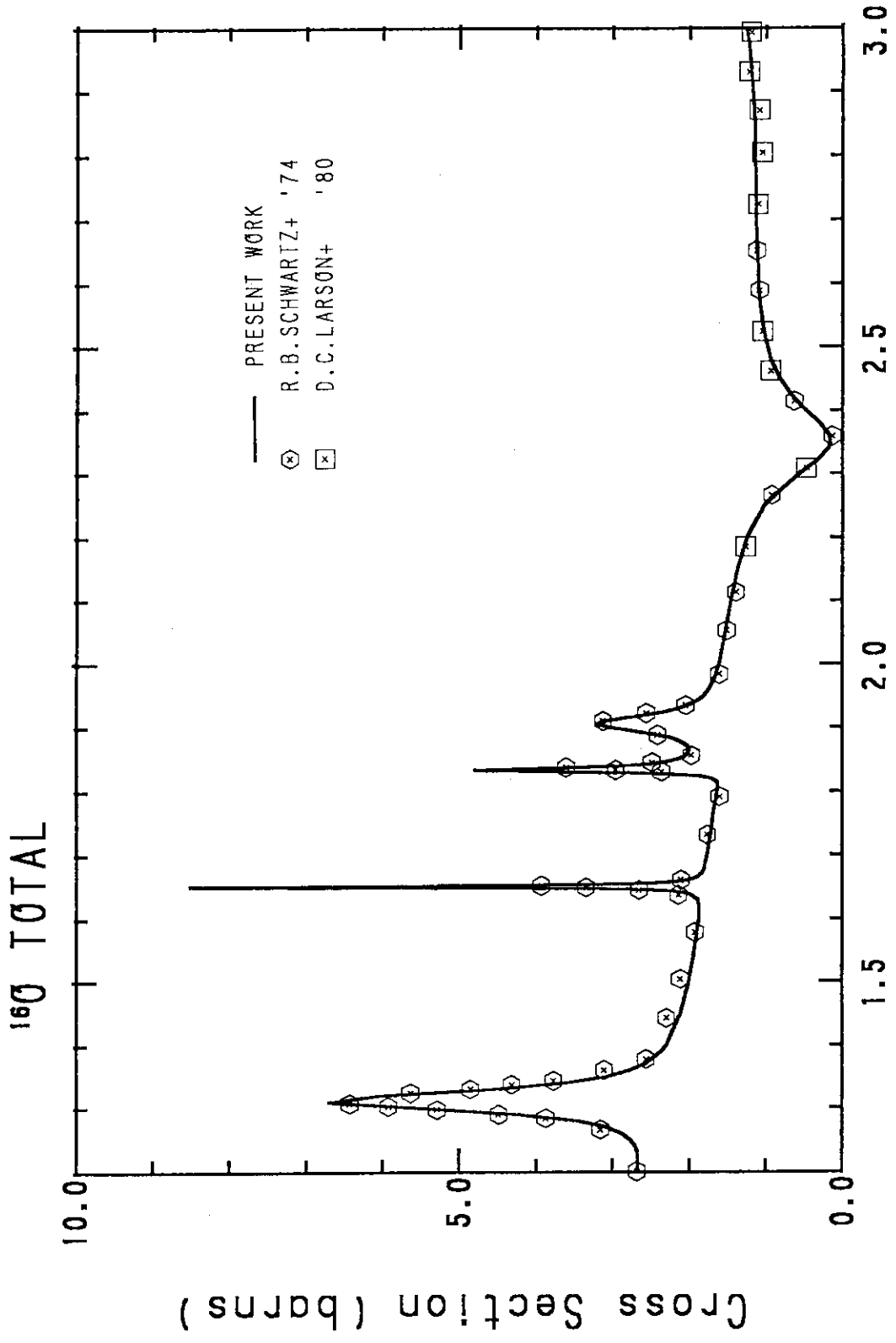

Fig. 2 Measured and evaluated total cross sections of ^{16}O between 1.2 MeV and 3 MeV.

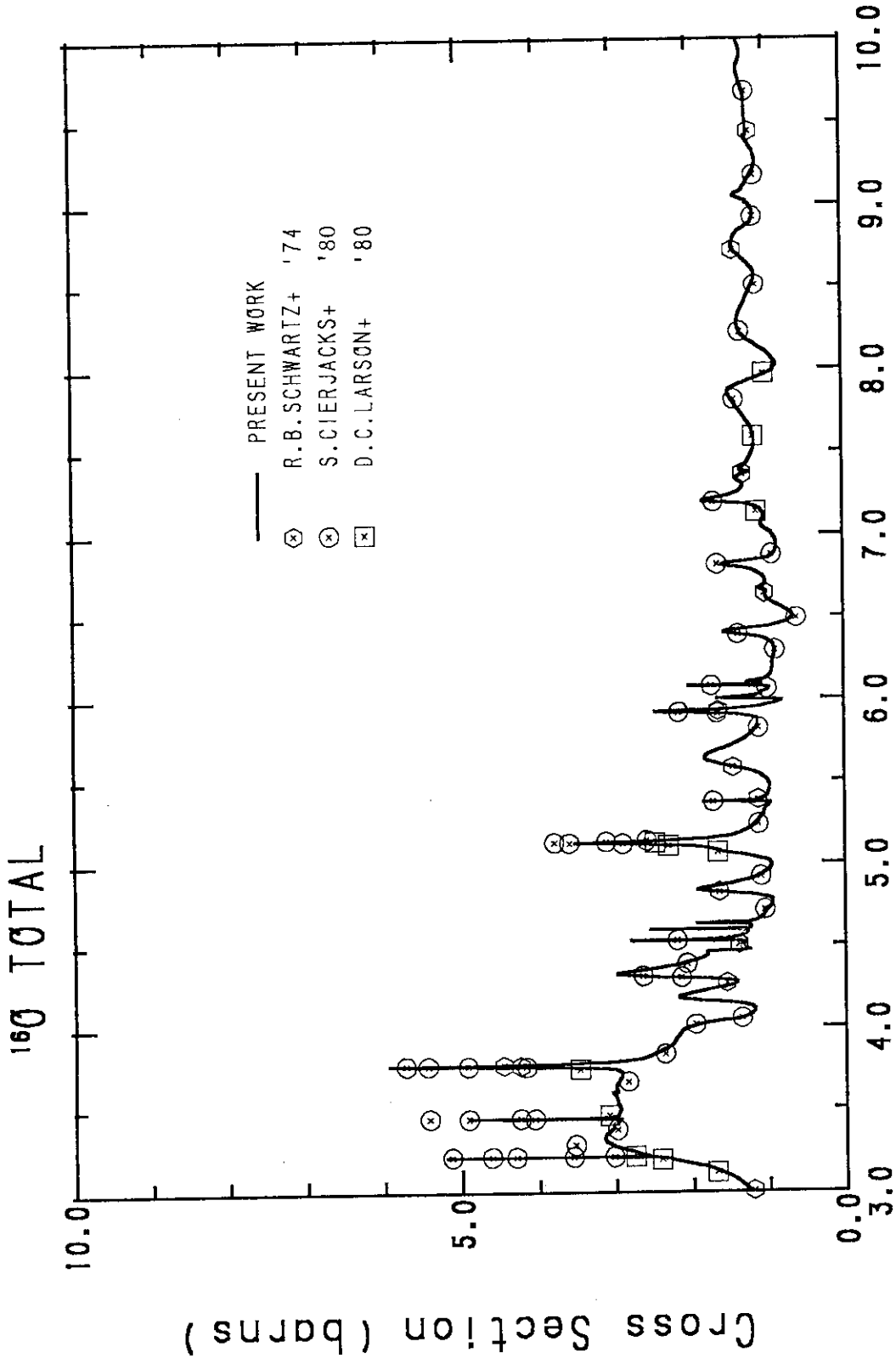

Fig. 3 Measured and evaluated total cross sections of ^{16}O between 3 MeV and 10 MeV.

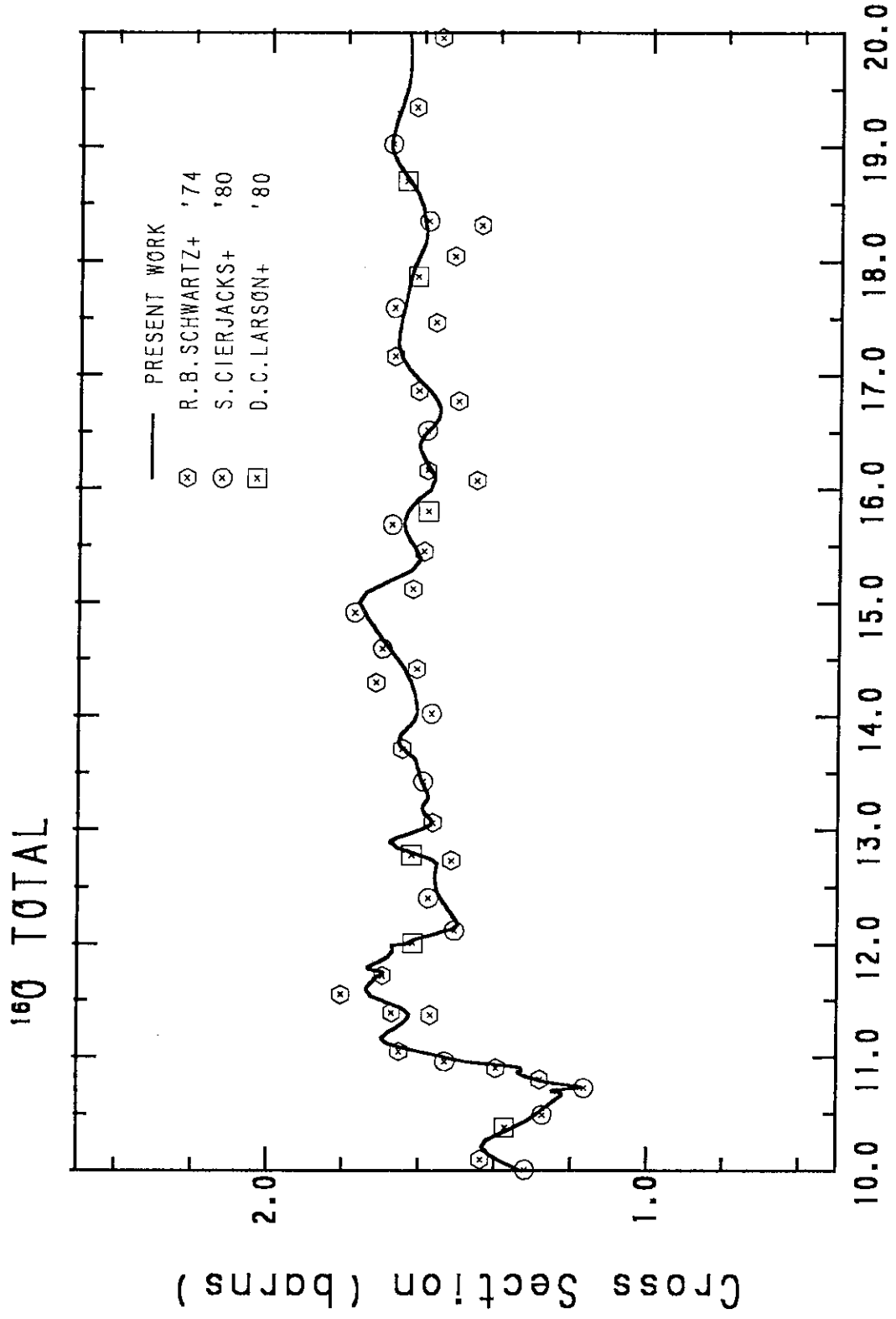

Fig. 4 Measured and evaluated total cross sections of ^{16}O above 10 MeV.

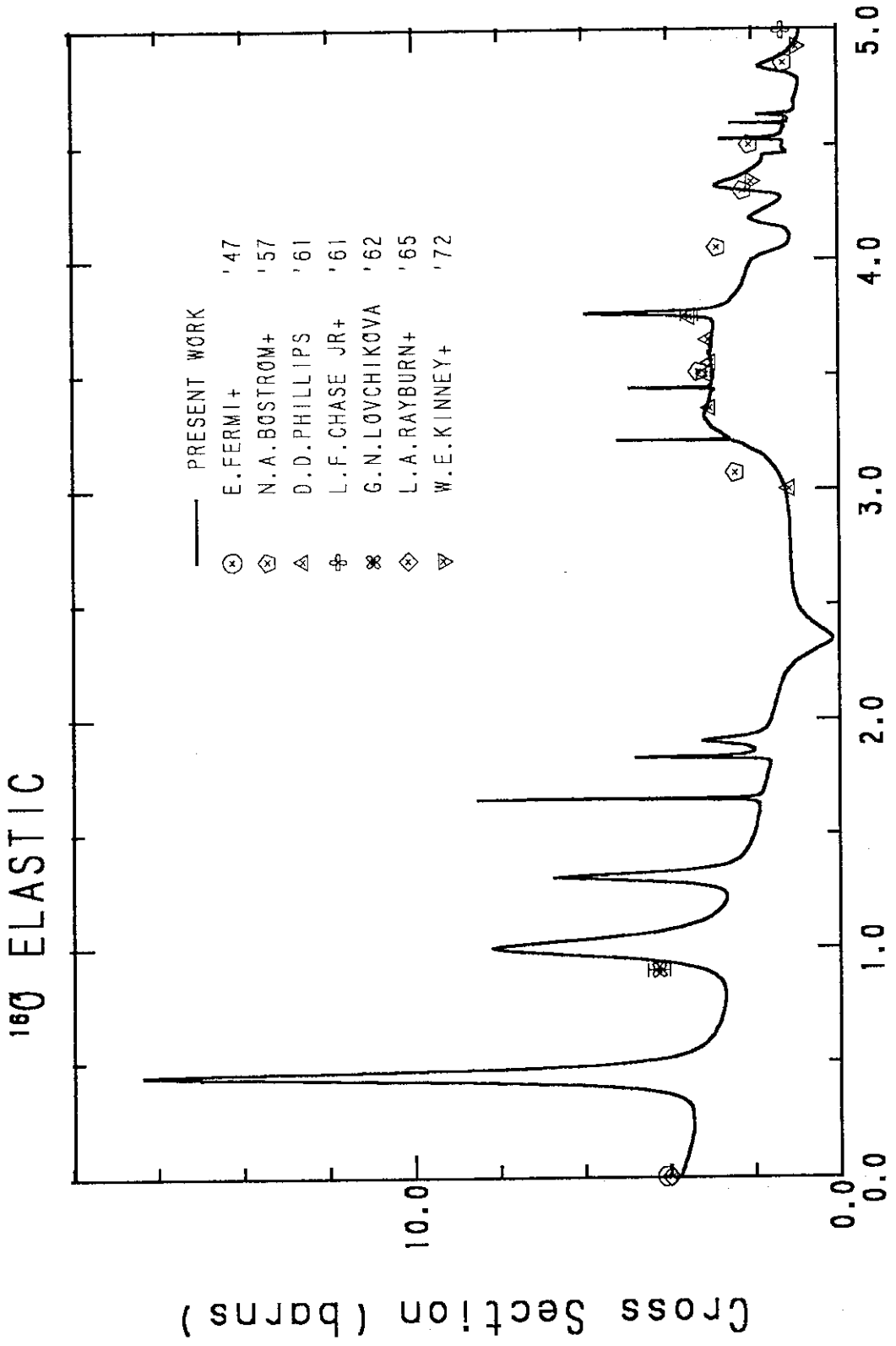

Fig. 5 Measured and evaluated elastic scattering cross sections of ^{16}O below 5 MeV.

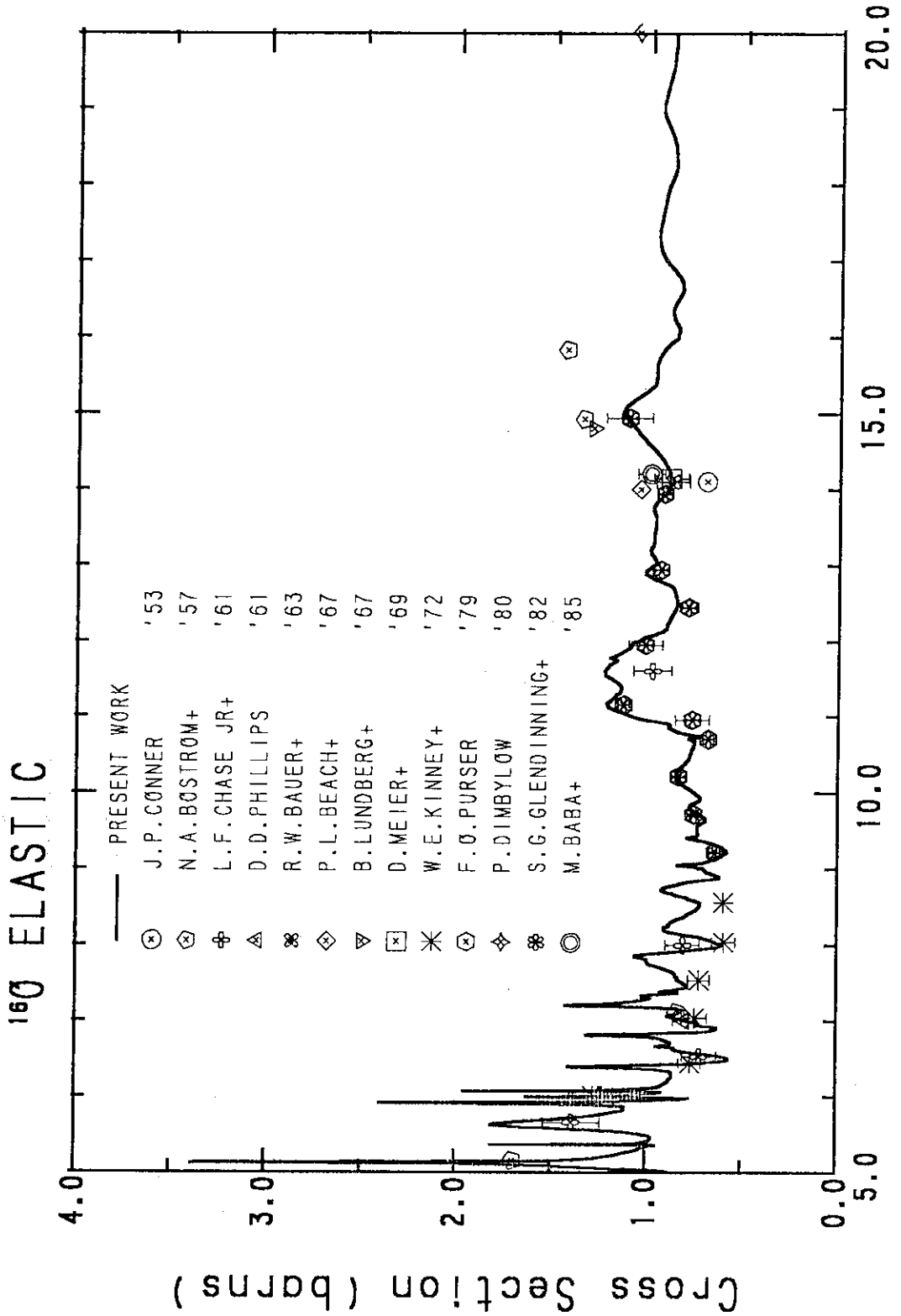

Fig. 6 Measured and evaluated elastic scattering cross sections of ^{16}O above 5 MeV.

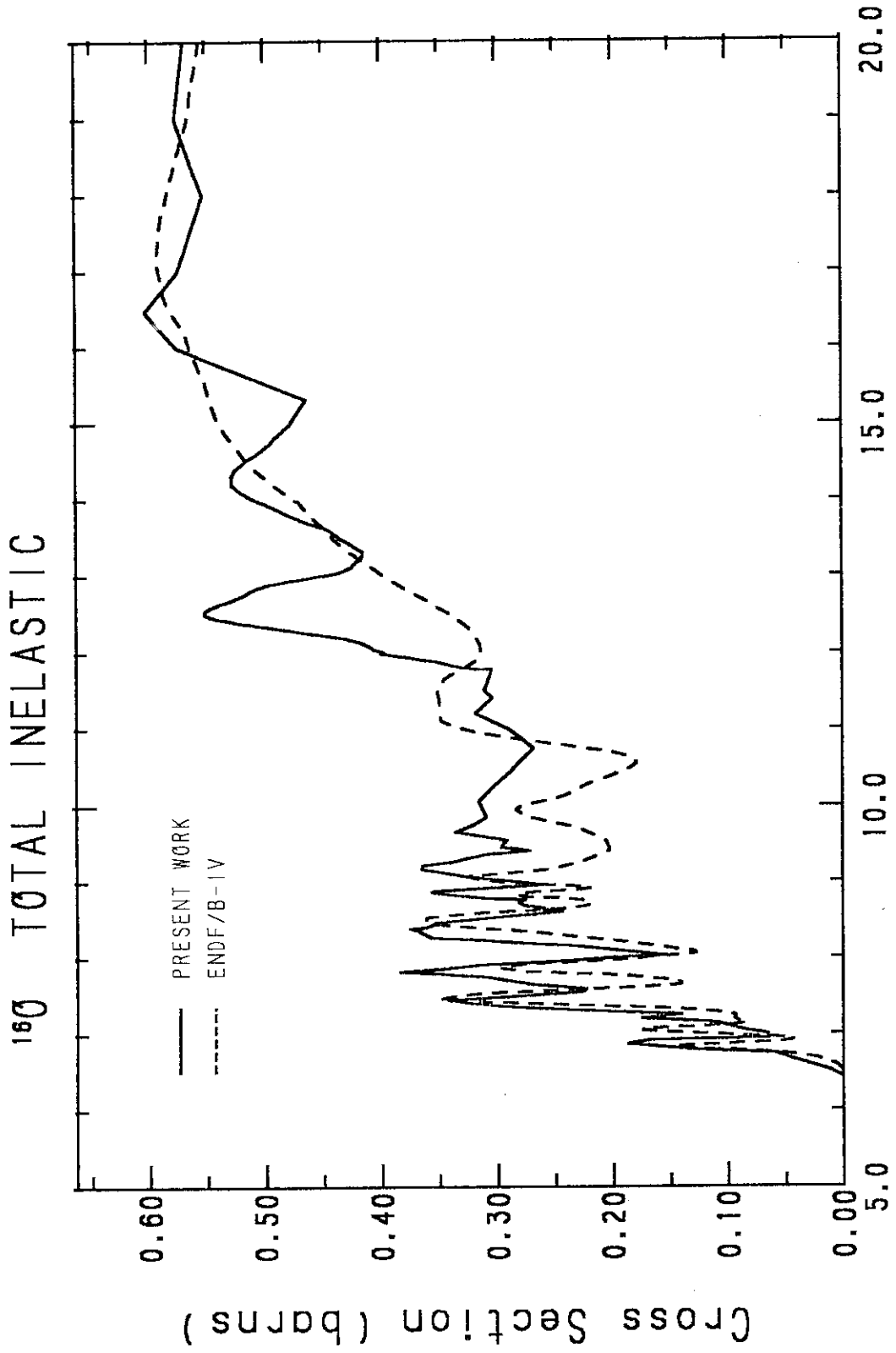

Fig. 7 Evaluated total inelastic scattering cross sections of ^{16}O.

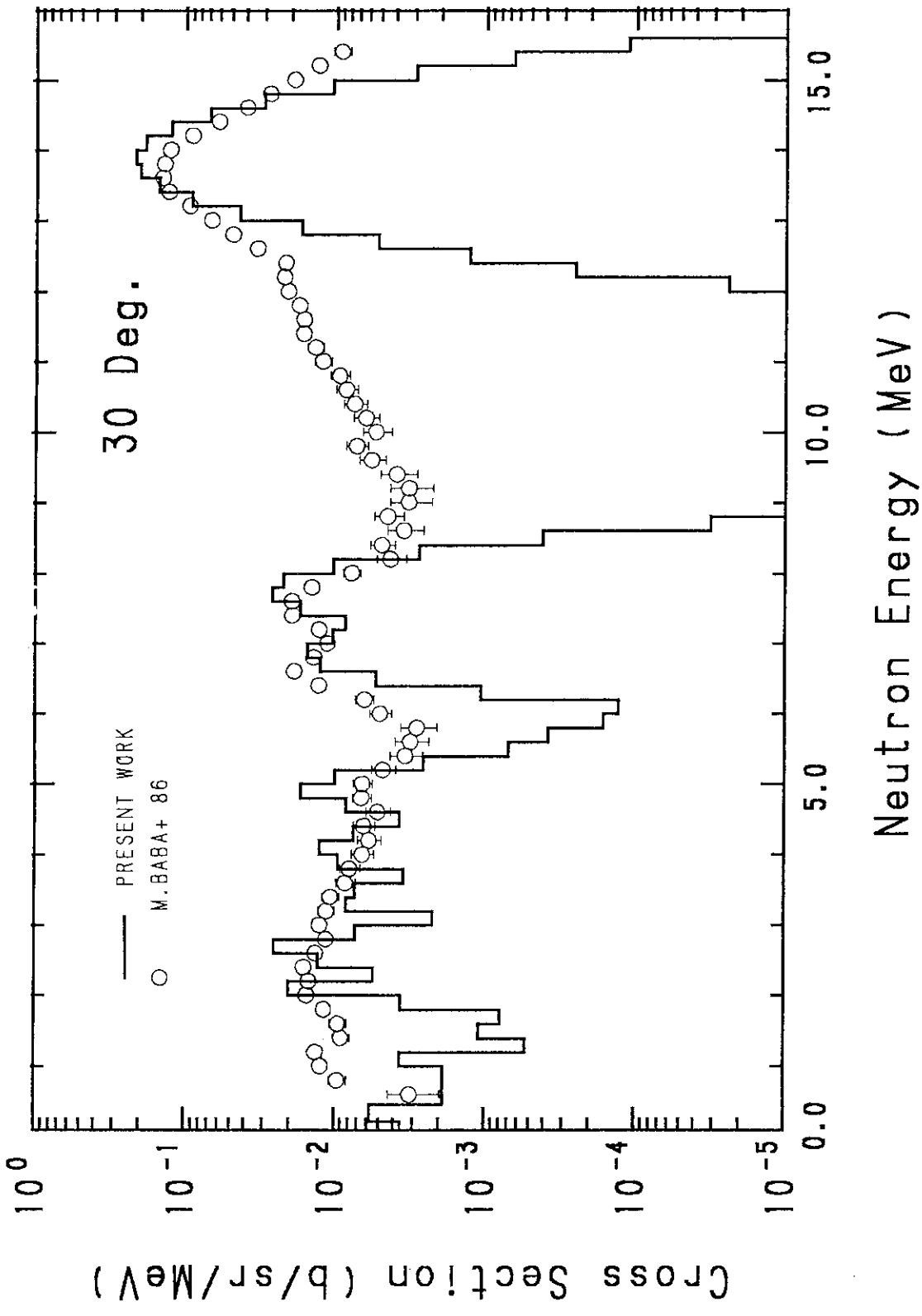

Fig. 8 Neutron emission spectra at 30 deg.

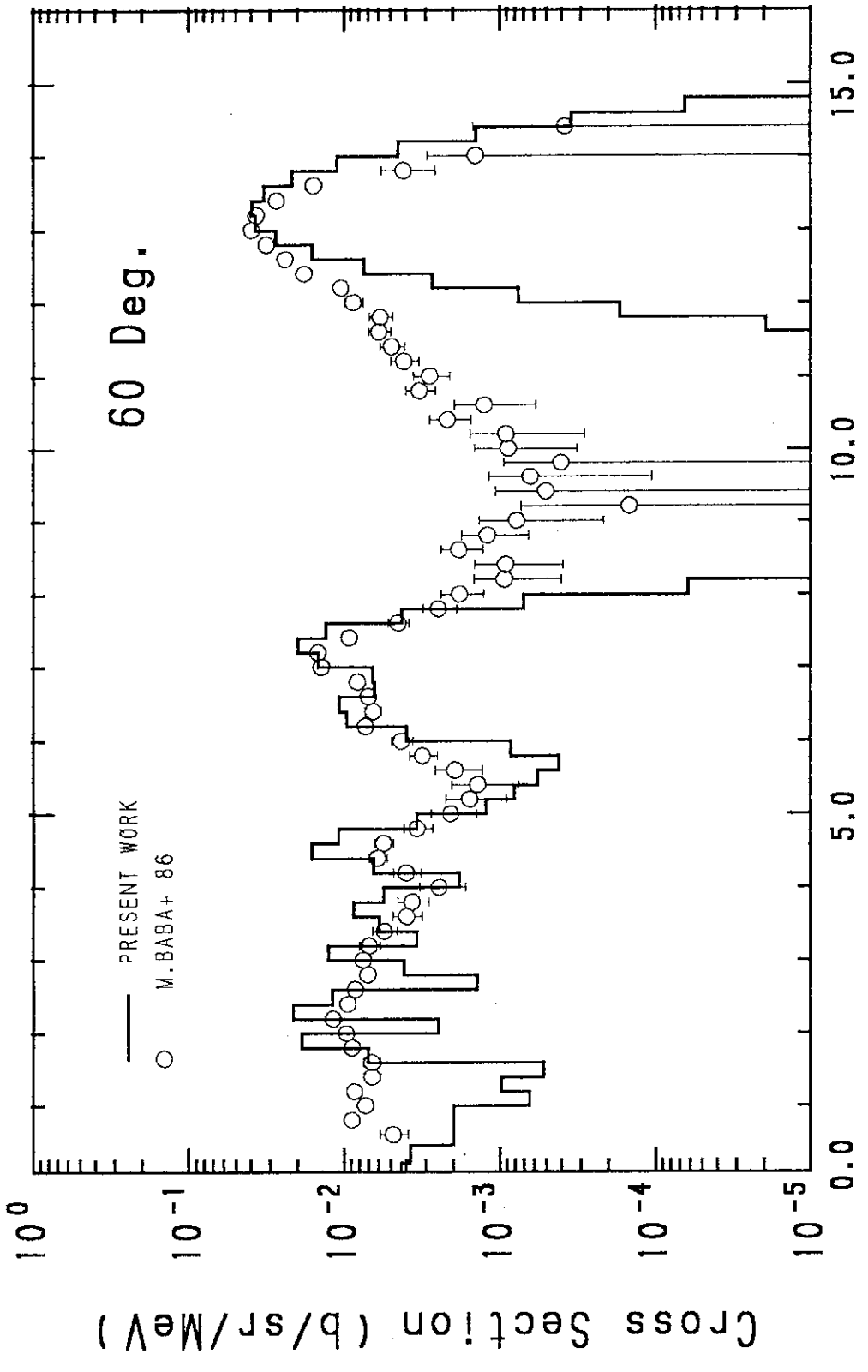

Fig. 9 Neutron emission spectra at 60 deg.

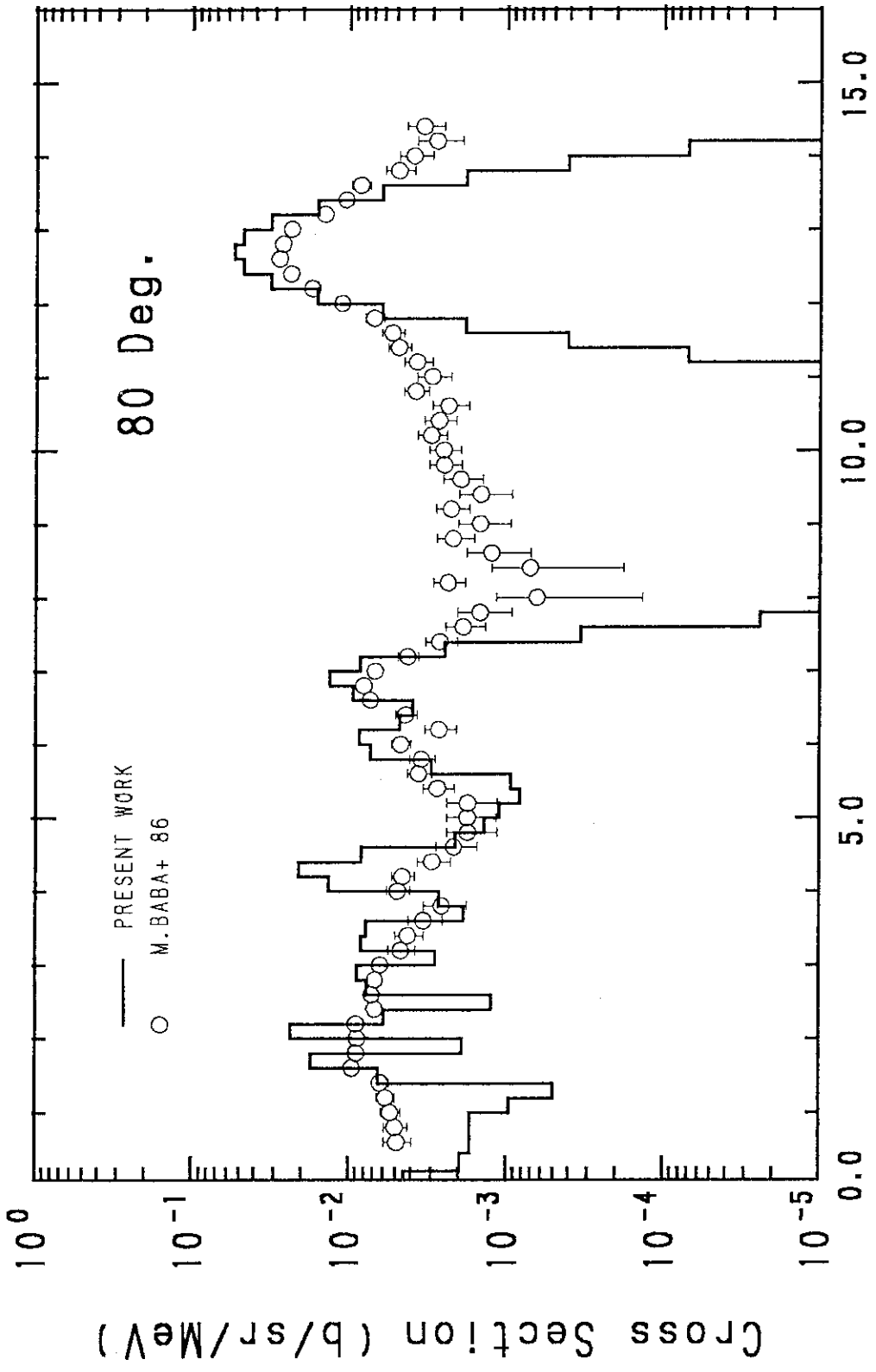

Fig. 10 Neutron emission spectra at 80 deg.

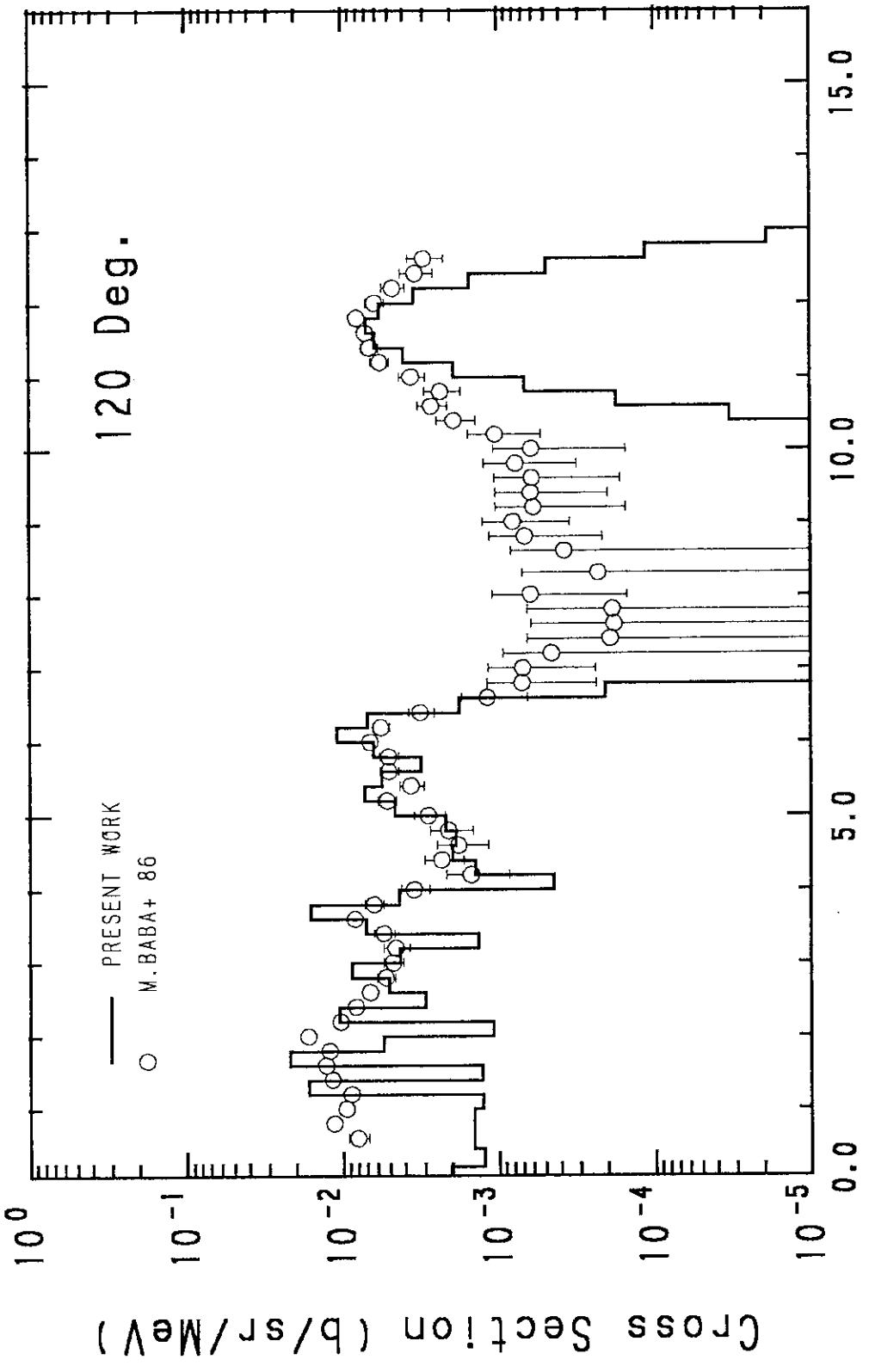

Fig. 11 Neutron emission spectra at 120 deg.

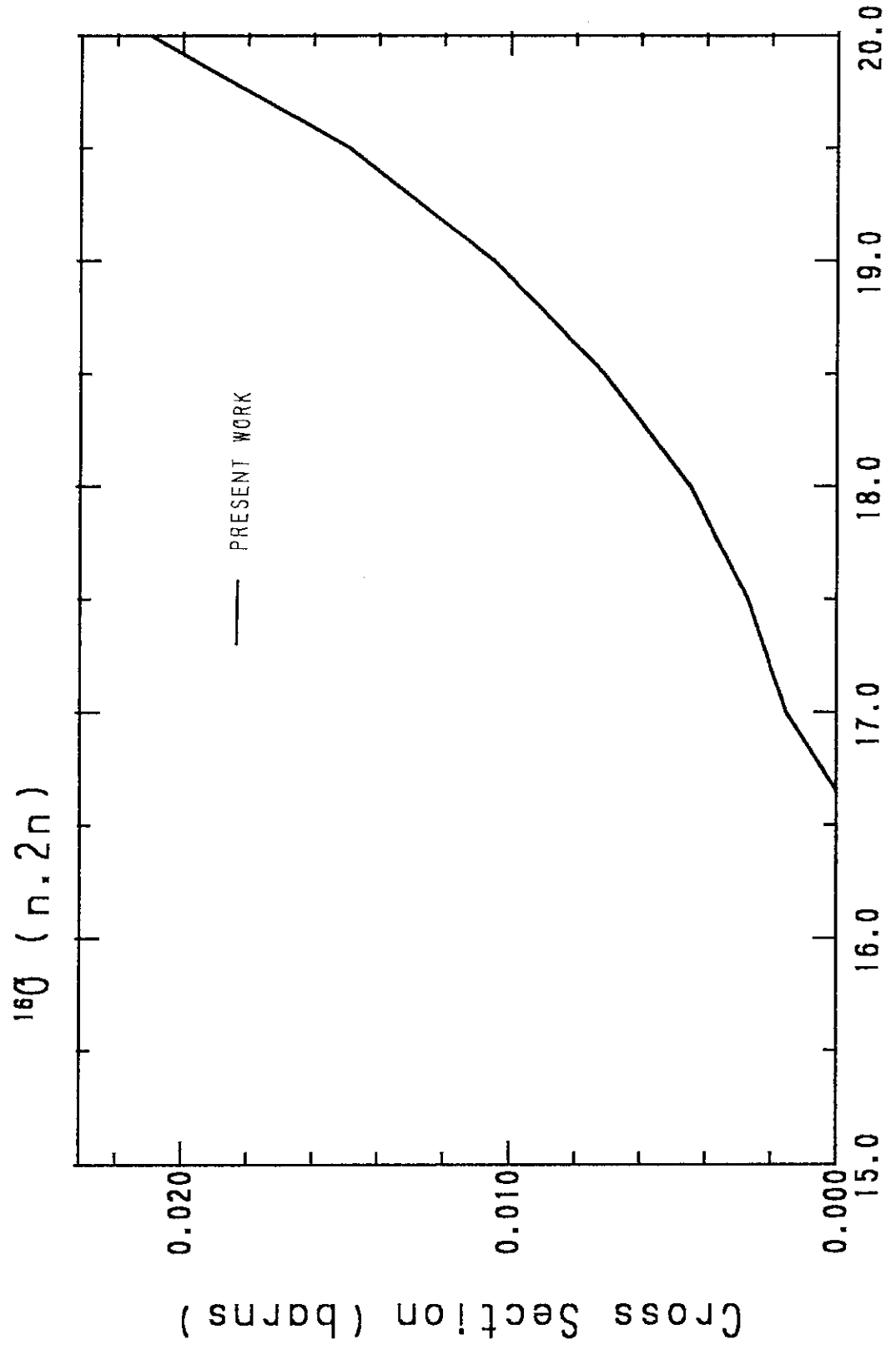

Fig. 12 Evaluated (n,2n) reaction cross section of ^{16}O.

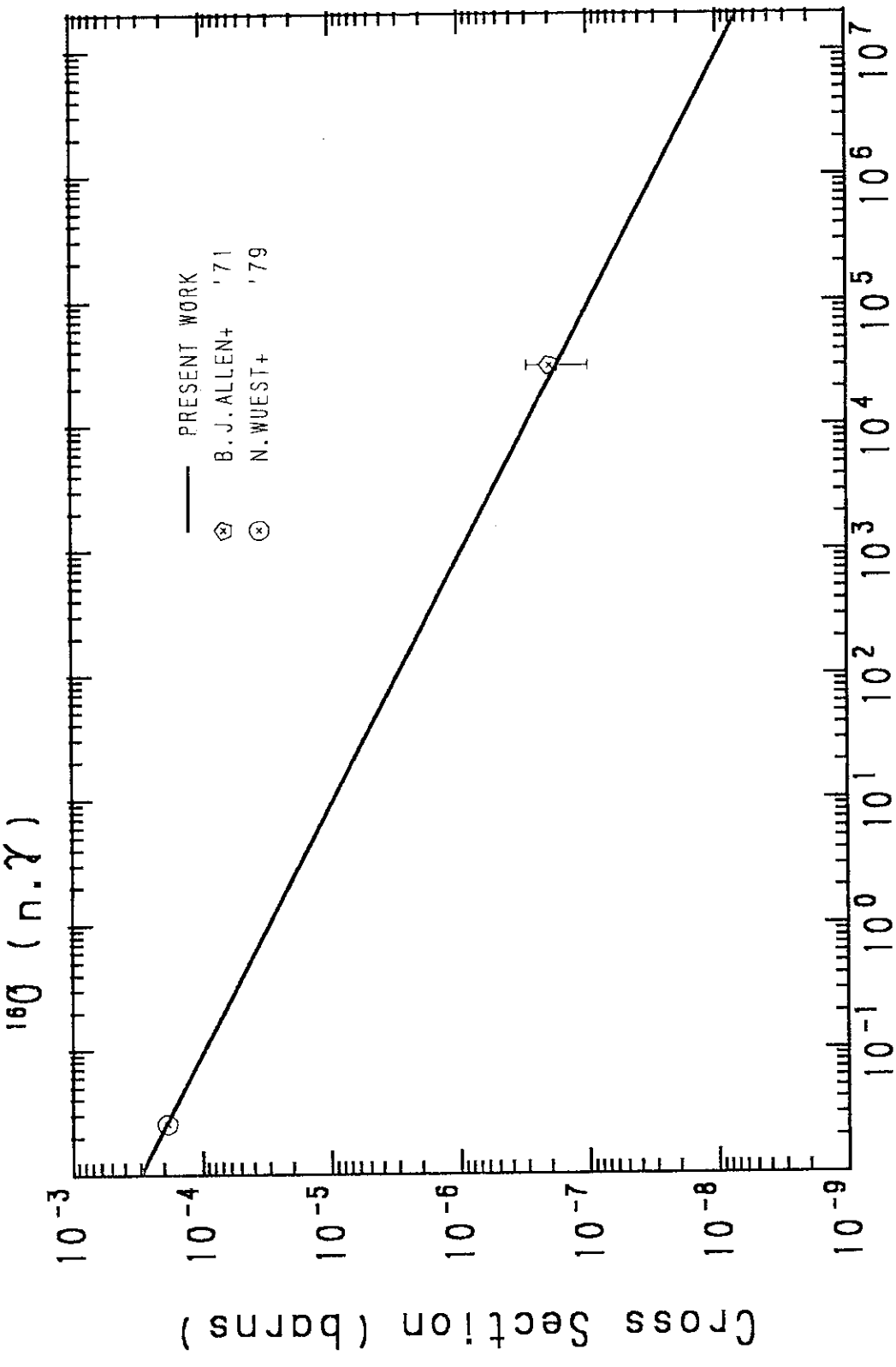

Fig. 13 Measured and evaluated (n,γ) reaction cross sections of ^{16}O.

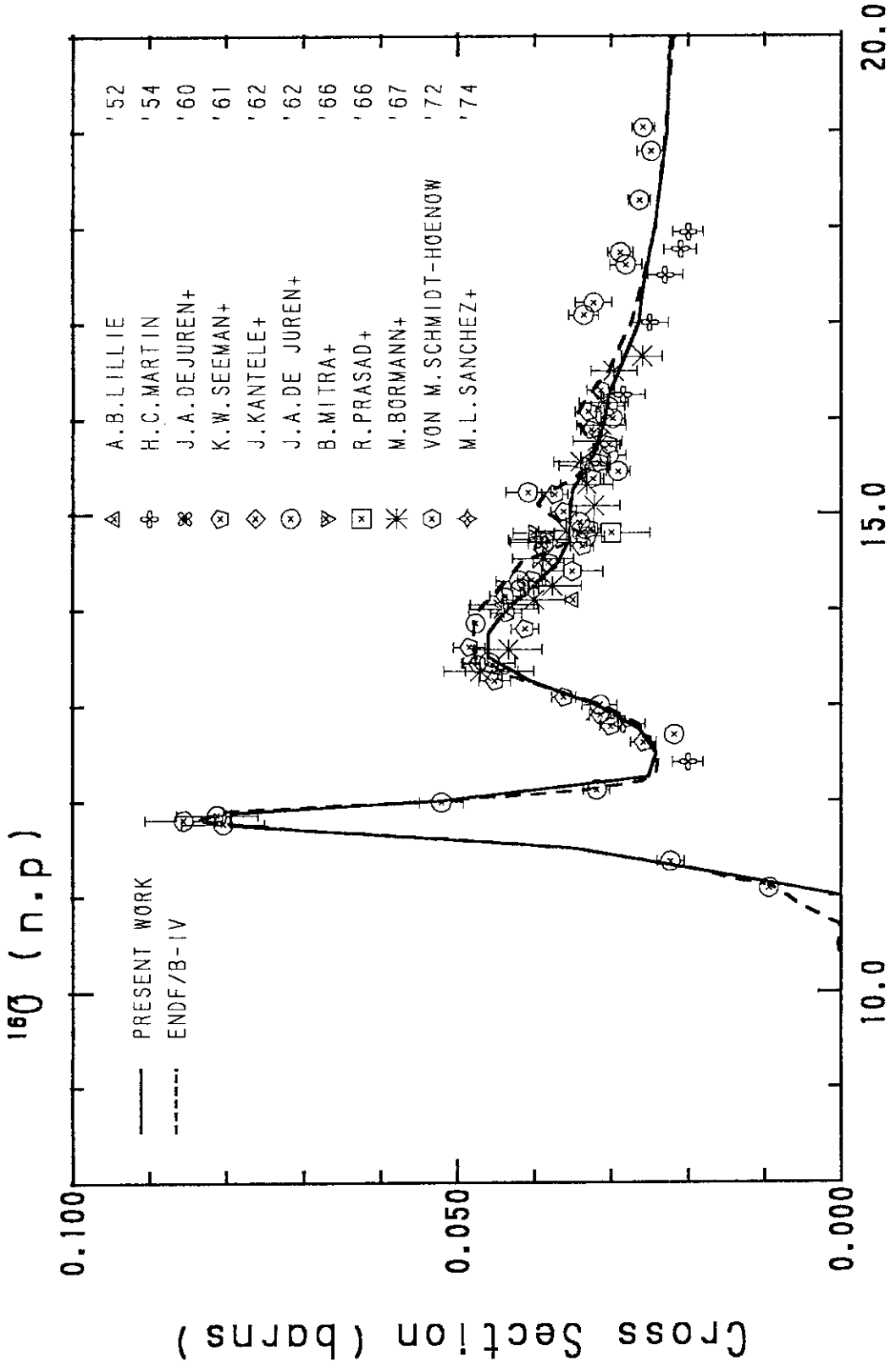

Fig. 14 Measured and evaluated (n,p) reaction cross sections of ^{16}O.

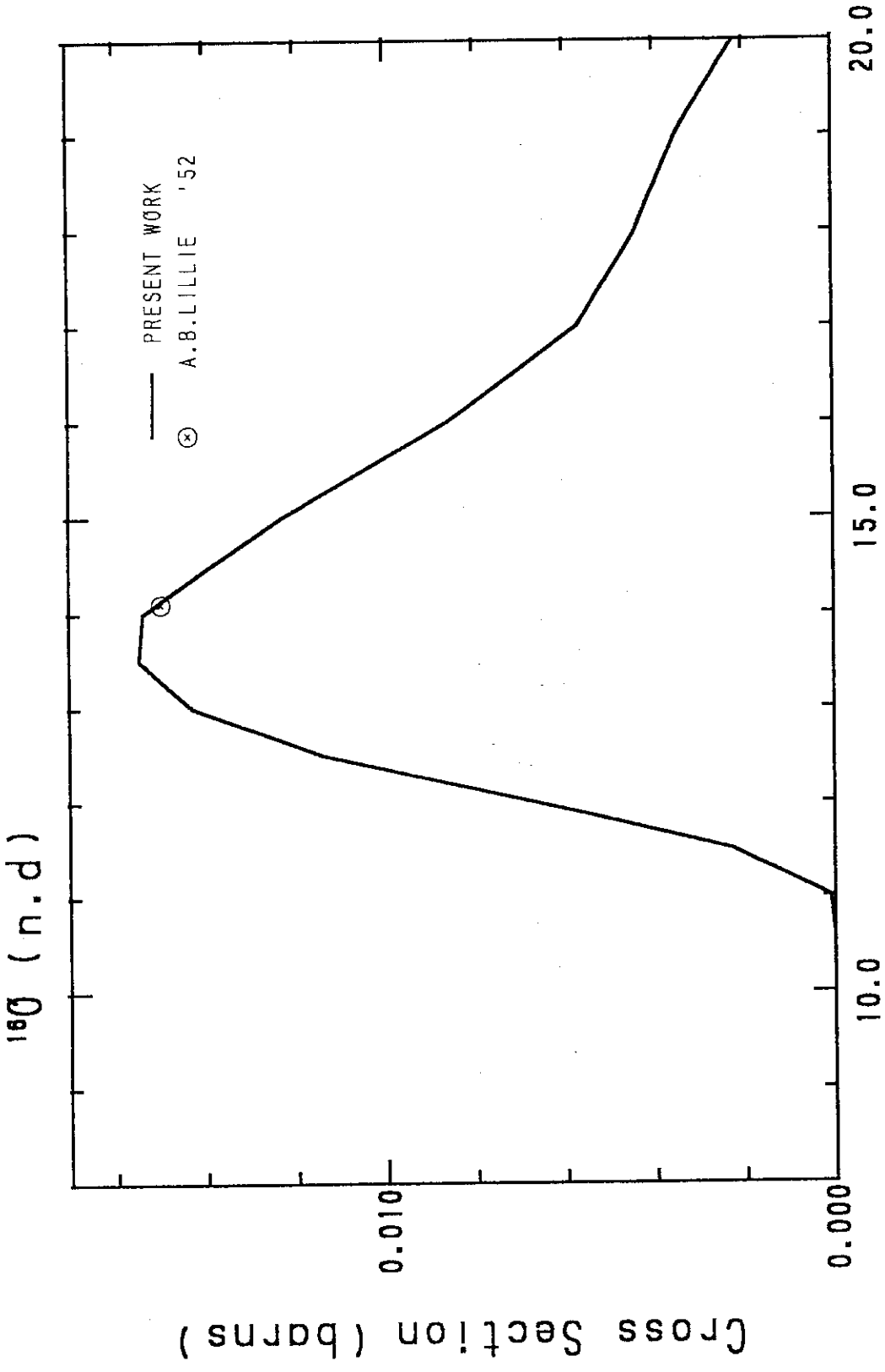

Fig. 15 Measured and evaluated (n,d) reaction cross sections of ^{16}O.

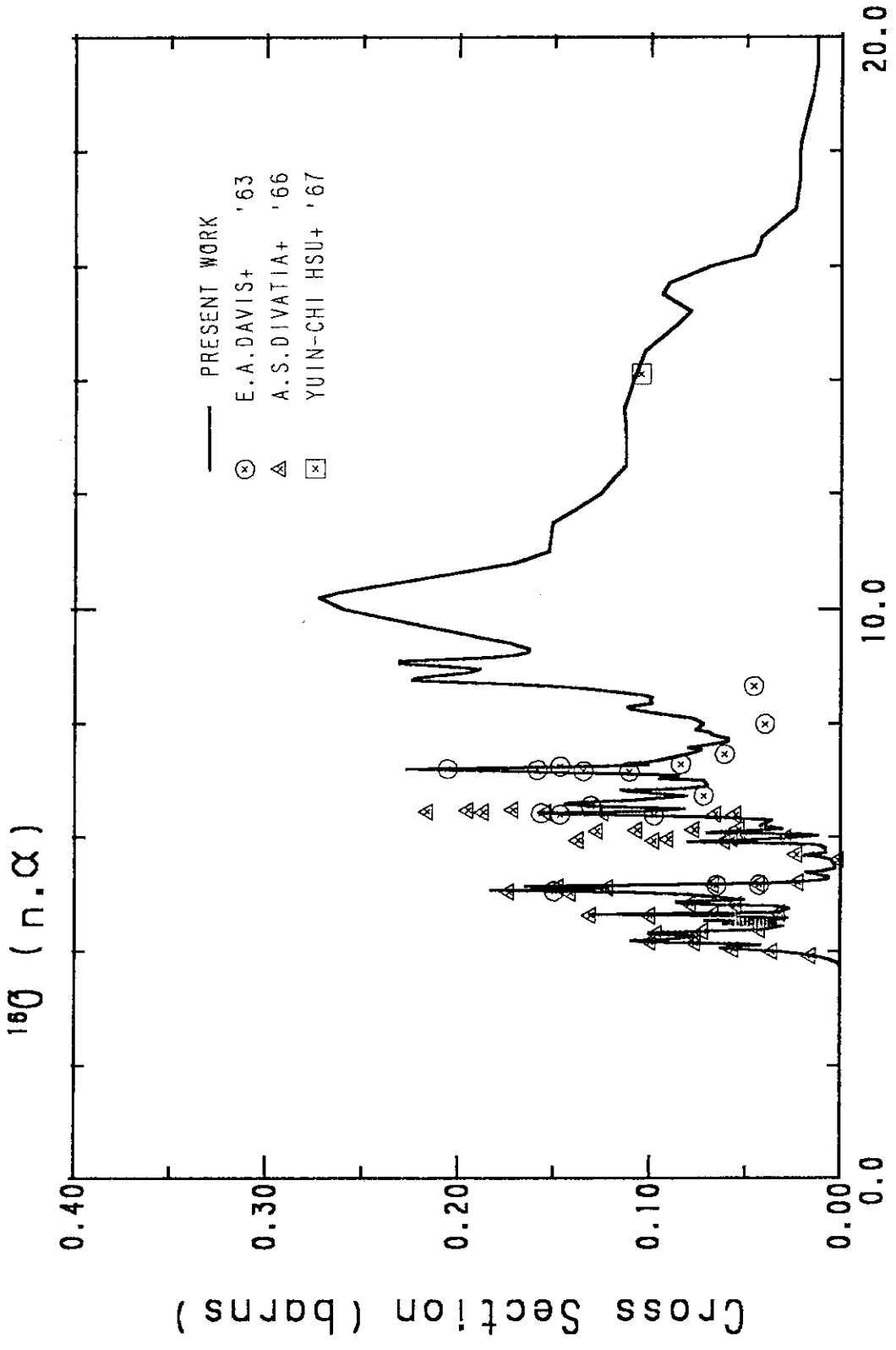

Fig. 16 Measured and evaluated (n,α) reaction cross sections of ^{16}O.

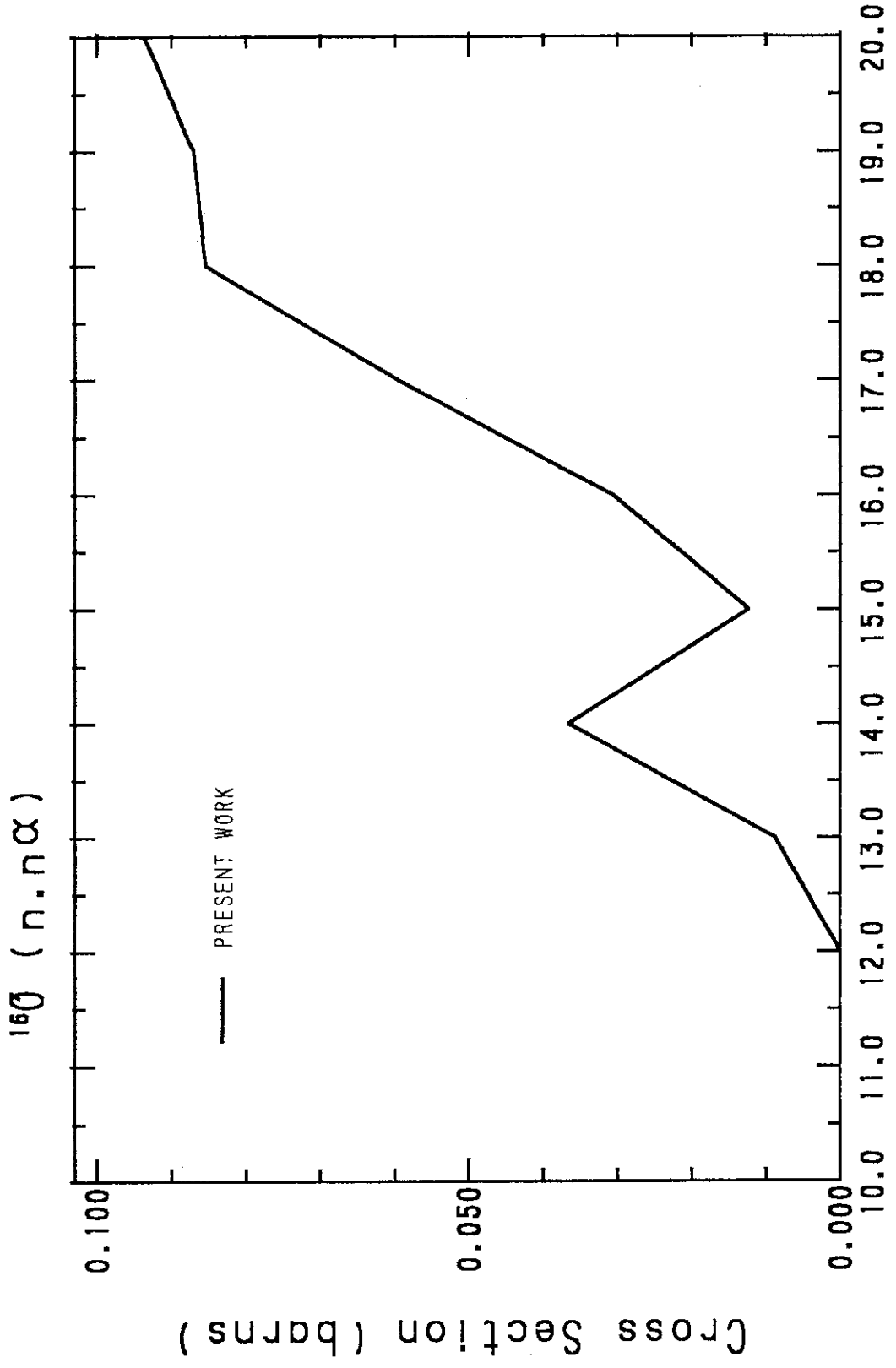

Fig. 17 Evaluated (n,nα) reaction cross section of ^{16}O.

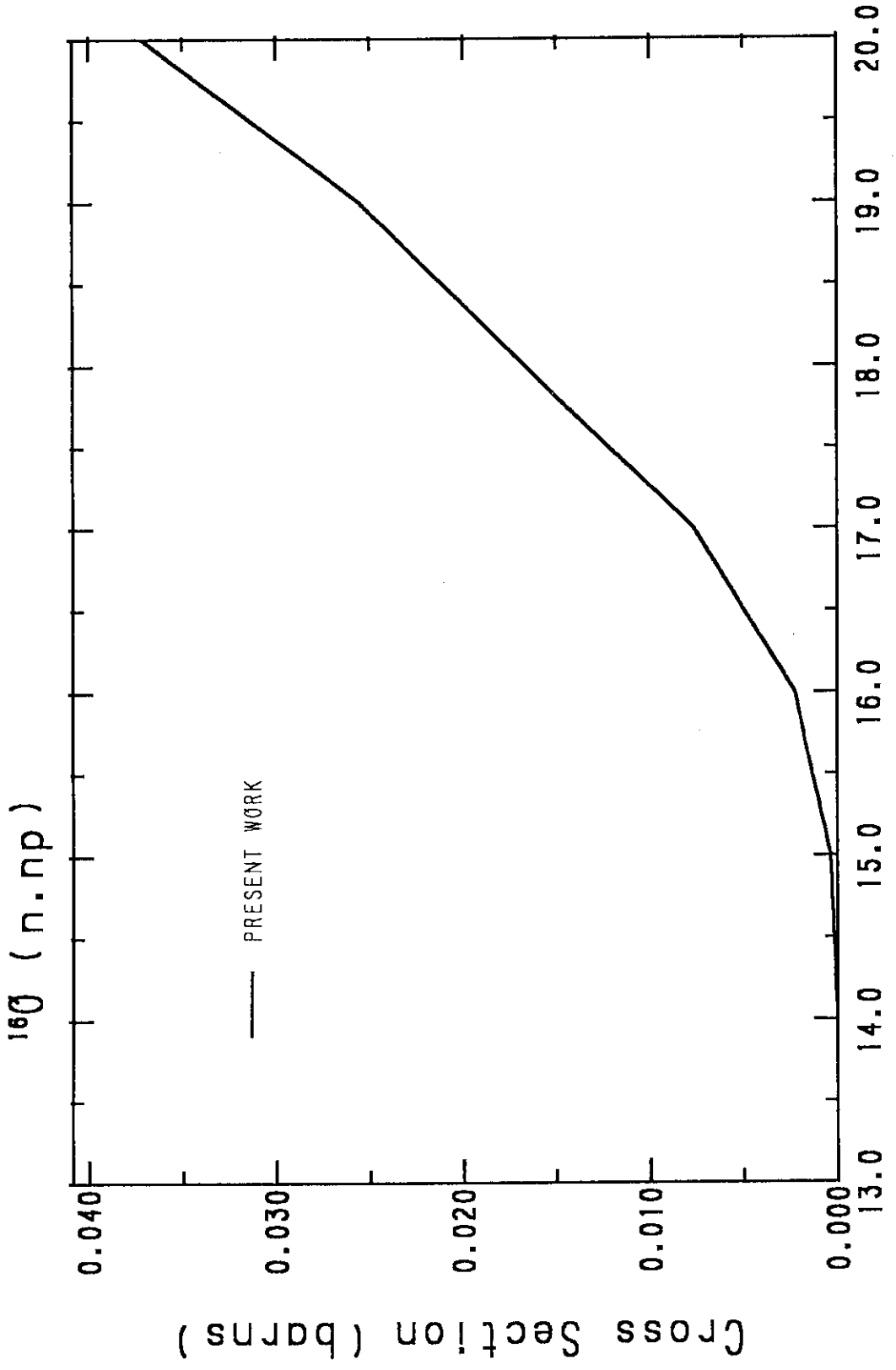

Fig. 18 Evaluated (n,np) reaction cross section of ^{16}O.